

Temporal shifts in displacement vectors: new insights into the unprecedented Mayotte volcanic event through advanced GNSS analysis

Atinc Pirti*, Secil Karatay

Pirti, A., Karatay, S. 2025. Temporal shifts in displacement vectors: new insights into the unprecedented Mayotte volcanic event through advanced GNSS analysis. *Baltica* 38 (1), 65–80. Vilnius. ISSN 1648-858X.

Manuscript submitted 1 October 2024 / Accepted 28 April 2025 / Available online 9 June 2025


© Baltica 2025

Abstract. The Mayotte seismic-volcanic crisis, initiated in May 2018, represents one of the most significant submarine magmatic events ever monitored in near real-time. This study leverages a nine-year Global Navigation Satellite System (GNSS) time series (2014–2023) from the MAYG station to investigate the temporal evolution and directional changes in ground displacement vectors associated with the event. Using both static and kinematic GNSS processing, including Precise Point Positioning with Ambiguity Resolution (PPP-AR), we identify three distinct phases of deformation: a north-eastward pre-crisis trend, an abrupt eastward shift coinciding with the peak magmatic activity (May 2018 – June 2019), and a post-crisis return to north-eastward motion with diminished but ongoing subsidence. The data reveal a dramatic 20 cm vertical subsidence and significant horizontal movement indicative of deep magma withdrawal and crustal readjustment. High-resolution analyses during the initial five days of the crisis suggest a sequence of discrete magmatic pulses. Our findings provide new insights into the geophysical response of volcanic island settings to deep-seated submarine eruptions and highlight the importance of integrating advanced GNSS techniques in understanding complex crustal deformation processes.

Keywords: GNSS deformation monitoring; submarine volcanism; Mayotte seismic-volcanic crisis; displacement vector analysis; PPP-AR geodetic technique

✉ Atinc Pirti* (atinc@yildiz.edu.tr),  <https://orcid.org/0000-0001-9197-3411>;

Department of Geomatic Engineering, Yildiz Technical University, 34220 Istanbul, Turkey;

Secil Karatay (skaratay@kastamonu.edu.tr),  <https://orcid.org/0000-0002-1942-6728>;

Department of Electrical Electronics Engineering, Kastamonu University, Kastamonu, Turkey

*Corresponding author

INTRODUCTION

Initially, both constructive processes such as lava flows, domes and pyroclastic deposits and destructive processes such as flank failure and caldera formation of volcanic eruptions can significantly alter the landscape by destroying vegetation and altering the porosity of the surface permeability and chemistry. These eruptions may be subtle, barely perceptible, or powerful, devastating the surrounding area. Volcanoes also alter the surface of the world by creating mountains, islands, and useful igneous materials. They also cause destructive natural disasters includ-

ing landslides (Noviyanto *et al.* 2020; Necmioglu *et al.* 2023), erosion (Neris *et al.* 2023; Yunita *et al.* 2024), floods (Vij 2022; Dolchinkov 2024) and tsunamis (Omira *et al.* 2022; Fan *et al.* 2024). The earth's surface may break due to the movement of the tectonic plates beneath it. These movements can cause this type of earthquakes of magnitude 2 or 5, which can be extremely slight or significant (Nagashima *et al.* 2023; Yao, Yang 2023). Diverging tectonic plates frequently lead to the formation of volcanoes as magma from the mantle rises through fissures, creating volcanic structures on land or in the sea (Bertil *et al.* 2021; Retailleau *et al.* 2022; Mercury *et al.* 2023).

Mayotte Island experienced an unparalleled seismic catastrophe with almost 300 earthquakes registered every day at the start of the crisis. Most of these earthquakes had a magnitude of less than 2.0; however, a few with a magnitude of between 3.5 and 5.9 were felt very intensely, frightening the populace (Mori 2021; Aiken *et al.* 2021; Devès *et al.* 2022). Mayotte is the oldest of the four large islands of the Comoros archipelago, a chain of land emerging from a crescent-shaped submarine relief at the entrance to the Mozambique Channel. Located 295 km west of Madagascar and 67 km southeast of Anjouan, sometimes visible at sunset in the shade, it is composed of several islands and islets covered with lush vegetation. Mayotte is a primarily volcanic island rising steeply from the bed of the ocean to a height of 660 metres on Mont Bénara. Two volcanic centres are reported, a southern one (Pic Chongui, 594 metres) with a breached crater to the NW, and a northern centre (Mont M'Tsapéré, 572 metres) with a breached crater to the south-east. Volcanic activity started about 7.7 million years ago in the south, ceasing about 2.7 million years ago. In the north, activity started about 4.7 million years ago and lasted until about 1.4 million years ago (Volcano Discovery 2004; Zinke *et al.* 2003). Both centres had several phases of activity. On 15 May 2018, an earthquake with magnitude M_w 5.9 occurred on the island. The epicentres of the earthquakes were distributed between 5 and 15 km east of the island, along an alignment of volcanic cones at 25 km east of the island, and at depths ranging from 25 to 50 km offshore east of Mayotte (Bertil *et al.* 2021; Retailleau *et al.* 2022; Devès *et al.* 2022; Mittal *et al.* 2022; Mercury *et al.* 2023).

In this study, the ground displacements measured by Global Navigation Satellite System (GNSS) stations have been examined for Mayotte seismic-volcanic crisis. Analysis in the study for ground displacements recorded by GNSS stations in connection with the ongoing seismic-volcanic crisis in Mayotte has revealed that ground deformation related to the current offshore volcanic activity east of Mayotte is either too low at this time to be detected in very far field, or it does not extend up to 250 km (Lemoine *et al.* 2020; Liuzzo *et al.* 2021; Foix *et al.* 2021; Lacombe *et al.* 2024). Lemoine *et al.* (2020) characterized the beginning and the course of a significant magmatic event by comparing the seismicity from the beginning of the crisis to its first year with ground deformation observations by GNSS and InSAR (Interferometric Synthetic Aperture Radar) and modelling. A 20 km range of potential models has been observed along the longitude axis, notwithstanding the robustness of the ground deformation modelling because of the unusual design of the GNSS stations. Mori (2021) has examined accounts of an extraordinary earth-

quake outbreak that the people living on the island of Mayotte in the Mozambique Channel witnessed. Using the threshold chronotope, stories in this study have been examined in terms of liminality, assessment, and (dis)placement in time. The analysis of the data collected from the on-land GNSS network (Peltier *et al.* 2022) and their modelling were combined with data from ocean bottom pressure gauges. A maximum of approximately 25 cm of cumulative eastern on-land ground displacement and a maximum of approximately 19 cm of subsidence were noted between July 2018 and the end of 2020. The decline in the flow estimated by the bathymetric survey, which drops from 172–181 m^3/s in the first year to less than 11 m^3/s by the end of 2020, was consistent with the decrease in the flux inferred from the inversion of ground deformation in this study (Peltier *et al.* 2022). Saurel *et al.* (2022) routinely has processed the data retrieved from the Ocean Bottom Seismometers in order to better pinpoint the position of the daily earthquakes that the land network observed. First, they have developed a novel 1-D local velocity model and set up particular data processing protocols. Between February 2019 and May 2020, they manually selected over 125,000 P and S phases from land and marine bottom stations in order to identify over 5000 events. The earthquakes outline two separate seismic clusters offshore that are named proximal and distal. It has been observed that the proximal cluster is a cylindrical structure that is 20–50 km deep and is situated 10 km offshore the eastern beaches of Mayotte. The distal cluster stretches from 50 to 25 km deep beneath Mayotte's new volcanic structure, starting 5 km east of the proximal cluster (Saurel *et al.* 2022). The differences of this study from other studies are that the horizontal movement that started at the Mayotte (MAYG) station in 2014 was in the north-east direction, while it turned towards the east direction as of May 2018, and this movement continued until June 2019. As of June 2019, the movement in the north-east direction continued until 2023. In addition, a collapse of approximately 20 cm was computed in the height differences from May 2018 to June 2019. Especially, when the obtained differences between kinematic and static GNSS processing were examined, it was clearly observed that the largest horizontal and vertical deformations occurred in 2018. The developed model and data and the results are given in Sections 2 and 3, respectively.

The unprecedented nature of the Mayotte seismic-volcanic crisis presents a unique opportunity to investigate the dynamics of underwater volcanic systems and their associated tectonic interactions. This crisis, characterized by its longevity and intensity, has significantly contributed to our understanding of magmatic processes in the region. While previous

researches (Bertil *et al.* 2021; Jeanson *et al.* 2021; Roullé *et al.* 2022; Retailleau *et al.* 2022) have established correlations between seismic activity and ground deformation, less attention has been given to the temporal evolution of displacement vectors and their directional changes over extended periods. The shift in horizontal movement direction at the MAYG station – from northeast to east and back to northeast – suggests complex underlying magmatic processes that warrant further investigation (Feuillet *et al.* 2021). Recent technological advancements in geodetic monitoring systems have enabled more precise measurements of ground deformation patterns. The integration of satellite-based observations with terrestrial monitoring networks provides comprehensive datasets that capture both the spatial extent and temporal evolution of these deformations (Shults *et al.* 2023; Fabris, Floris 2023; Gagliardi *et al.* 2023; Tan *et al.* 2023). Our study leverages these technological capabilities to analyze the subtle yet significant directional changes in ground movement that occurred between 2014 and 2023, with particular emphasis on the critical period from May 2018 to June 2019 when the most dramatic changes were observed. Understanding the mechanisms driving these directional shifts in ground movement is crucial for developing more accurate predictive models of volcanic behaviour in island settings. The Mayotte case presents distinct characteristics compared to other volcanic islands, as the observed deformation patterns appear to be linked to deep magmatic processes occurring at unusual depths (25–50 km). By comparing the kinematic and static GNSS processing results (Bousquet *et al.* 2020), the specific forces driving these directional changes and quantifying their magnitudes have been identified in this study with a greater precision than in previous studies.

This research contributes to the growing body of knowledge on submarine volcanic systems and their impacts on island stability. The findings have implications not only for understanding the geological evolution of the Comoros archipelago but also for improving risk assessment and hazard mitigation strategies for populations living in volcanic island environments worldwide. By establishing a more detailed chronology of deformation events and correlating them with seismic activity, a foundation for future research into the complex interplay is provided between magmatic processes and crustal deformation in oceanic settings.

DESCRIPTION OF THE STUDY AREA

Mayotte is a primarily volcanic island rising steeply from the bed of the ocean to a height of 660 metres on Mont Bénara. Two volcanic centres are re-

ported, a southern one (Pic Chongui, 594 metres, with a breached crater to the NW, and a northern centre (Mont M'Tsapéré, 572 metres) with a breached crater to the south-east. Mont Bénara is between these two peaks, approximately at the contact point of the two structures. Volcanic activity started about 7.7 million years ago in the south, ceasing about 2.7 million years ago. In the north, activity started about 4.7 million years ago and lasted until about 1.4 million years ago. Both centres had several phases of activity. The 11 November 2018 seismic event occurred about 24 km off the coast of Mayotte. It was recorded by seismograms in many places, including Kenya, Chile, New Zealand, Canada and Hawaii located almost 18.000 km away. The seismic waves lasted for more than 20 minutes, but despite this, no one felt it. Subsequently, the earthquake swarm was linked to a newly discovered undersea volcano located 50 km away from Mayotte at a depth of 3.500 m. As part of the Comoro Islands chain in the Mozambique Channel, the geology of Mayotte is virtually the same as the geology of the Comoros, the rest of the island chain which is independent of France. The island resulted from the rifting of Madagascar away from Africa as well as “hotspot” mantle plume activity and is also impacted by seismicity and deformation associated with the East African Rift. However, because Mayotte is a part of France, its geology is significantly more researched than that of other islands in the chain. As with other islands in the Comoros chain, Mayotte’s location in the Mozambique Channel is tectonically complex due to the displacement of the Malagasarian microcontinent from the margin of the supercontinent Gondwana. Starting in May 2018, there have been many minor earthquakes under the eastern flank of the volcano constituting what is generally referred to as a “swarm” (Bertil *et al.* 2021; Retailleau *et al.* 2022; Mercury *et al.* 2023). The exact nature of the forces behind this swarm remains unclear as of March 2019. The region used for the study was African Plate and IGS station MAYG (12.78°W, 45.25°E) (IGS, 1994).

The earthquake swarm began east of Mayotte on 10 May 2018. The strongest quake (M 5.9), the largest-magnitude event ever recorded in the Comoro zone, struck on 15 May 2018. The swarm includes thousands of quakes, many of them felt by Maorais residents. Temporarily installed ocean-bottom seismometers showed that the swarm active zone was sited 10 km east of Mayotte (USGS 1879). Deep into the oceanic lithosphere (in the 20–50-km depth range), a rather surprising result was observed because the swarm was believed to be caused by the deflation of a magma reservoir located 45 km east of Mayotte at a depth of 28 km. Accordingly, an oceanographic campaign discovered in May 2019 a new submarine vol-

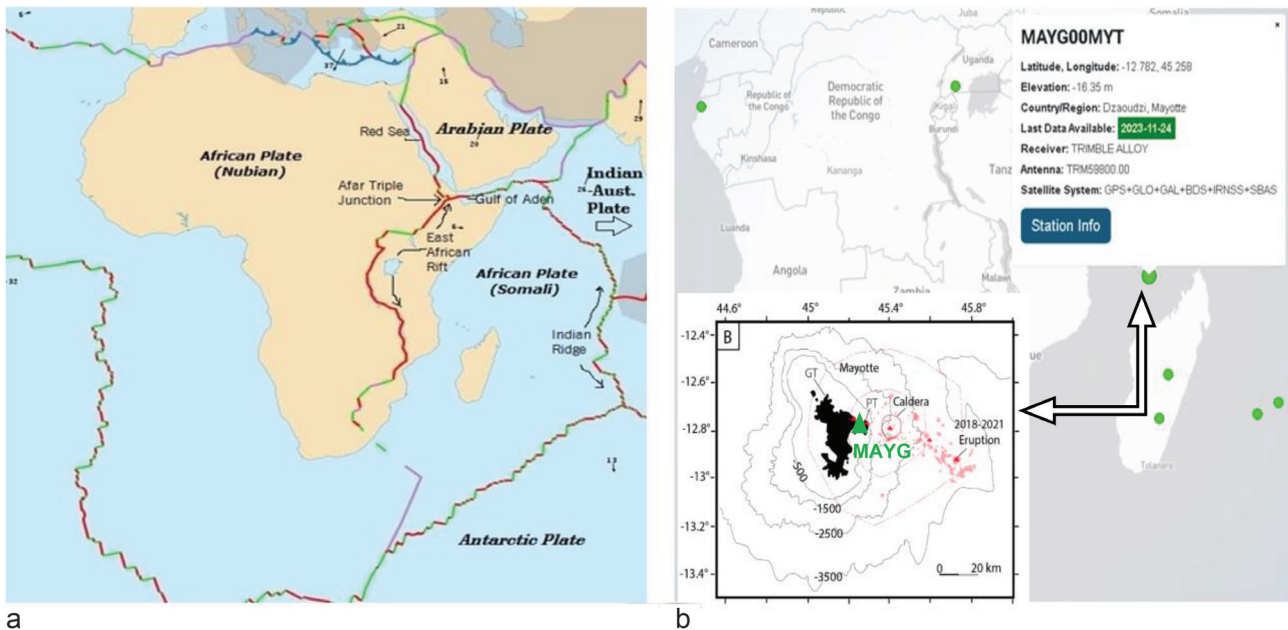


Fig. 1 The region chosen for the scope of the study: African Plate (Nubian and Somali Plate) (a) and IGS station MAYG in Indian Ocean (IGS, 1994) and Mayotte volcano (b)

cano, 800-m high and located 50 km east of Mayotte. The swarm had been tapering off between August and November 2018 when the 11 November 2018 event occurred. This event had no detectable P or S waves, but generated surface waves that could be observed worldwide by seismological observatories. Its origin is thought to be east of Mayotte. The swarm continued to be active all through 2019.

MATERIAL AND METHODS

GNSS Technology and Applications

The Global Navigation Satellite Systems (GNSS) technology is frequently deployed to measure various geophysical phenomena with high precision. These phenomena include tectonic plate movements (typically a few millimetres per year), volcano inflation and deflation cycles, and smaller-scale events such as landslides. One significant application of GNSS is determining earthquake magnitudes by surveying ground displacement at monitoring stations near fault lines. GNSS demonstrates particular value in measuring very large earthquakes, which can potentially trigger devastating tsunamis. For tsunami early warning systems, timely and accurate magnitude estimates are crucial. While seismometers offer greater sensitivity to ground movement, they often become saturated (“go off the scale”) during major seismic events, compromising their measurement accuracy. GNSS measurements, though less sensitive, do not suffer from this saturation limitation, making them reliable for large earthquake assessment. Between seismic events, GNSS networks can continuously

monitor the gradual deformation of the ground in plate boundary zones where earthquakes frequently occur. This monitoring capability allows scientists to estimate stress and strain accumulation on faults, contributing to improved seismic hazard assessments. Similarly, for volcanic activity, GNSS-surveyed surface displacements help estimate magma movement beneath the surface, providing valuable data for eruption forecasting.

Study Site Selection and Data Collection

The Mayotte volcanological and seismological monitoring network (REVOSIMA) documented 30,000 incidents from 25 February 2019 to 10 May 2020, derived from hand analysis of the continuous land data. In March 2019, one month after funding, four seismic stations were established onshore (three on Mayotte Island and one on Grande Glorieuse Island), and six Ocean Bottom Seismometers (OBS) were placed offshore within a 40 km radius of the seismically active region. A seismology team was established comprising researchers, engineers, and students from the participating French institutions: BRGM, Institut de Physique du Globe de Paris (IPGP), Institut Français de Recherche pour l’Exploitation de la Mer (IFREMER), and Institut National des Sciences de l’Univers du Centre National de la Recherche Scientifique (INSU-CNRS). In July 2019, the Mayotte seismo-volcanic monitoring network (Réseau de surveillance volcanologique et sismologique de Mayotte – REVOSIMA) was established in collaboration with all four universities. The team’s objective is to expedite the processing of freshly received data and to

achieve immediate findings in near real-time, thereby enhancing daily monitoring and understanding of the volcano-seismic situation (Saurel *et al.* 2022). Between May 2018 and June 2019, the Mayotte local real-time seismic network expanded from 1 to 8 stations. The research group has consistently modified daily data analysis techniques across many institutes to leverage the growing number of local stations and enhance event localisation accuracy. In 2019, there was established a novel approach to effectively handle OBS data during pickathons, whereby several analysts collaborate for several days on freshly recovered data (Saurel *et al.* 2022; Peltier *et al.* 2022; REVOSIMA 2019; Bhattacharya 2020).

Seismic activity that began in July 2018 (Cesca *et al.* 2020; Lemoine *et al.* 2020) and increased in intensity towards the end of August 2018 is correlated with the proximal cluster. According to GNSS data, this month marks the start of the island's subsidence and eastward displacement, which is thought to be caused by the draining of a magma chamber that is at least 30 km deep (Cesca *et al.* 2020; Lemoine *et al.* 2020; Feuillet *et al.* 2021). The Ministry of Environment (ministère de la transition écologique et solidaire – MTES), INSU, and CNRS provided funding for the Tellus SISMAYOTTE project (broadband land stations and first OBSs, MAYOBS1, doi:10.17600/18001217). With the assistance of DIRMOM (Direction Interministérielle aux Risques Majeurs en Outremer), the Ministère de la Transition Ecologique (MTE), the Ministère de l'Enseignement Supérieur, de la Recherche et de l'Innovation (MESRI), the Ministère des Outre-Mer (MOM), and the Ministère de l'Intérieur (MI) have been funding all of the activities on Mayotte since June 2019 (REVOSIMA 2019).

Since May 2018, the Comoros archipelago has undergone an unparalleled volcanic-seismic disaster. During the first year, many earthquakes were recorded east of Mayotte, the easternmost island in the archipelago, in an area that had previously shown seismic tranquillity (Bertil *et al.* 2021). The emergence of a new undersea volcanic structure with a volume of 6.55 km³ (Feuillet *et al.* 2021) necessitates a reevaluation of volcanic and seismic hazards in Mayotte. This reevaluation requires comprehension of the fundamental magmatic system. A data set that facilitates our comprehension of this system, originating from the onset of the crisis, is seismicity. Prior to the crisis, Mayotte had just one seismic station; nevertheless, the formation of the Réseau de surveillance volcanologique et sismologique de Mayotte (REVOSIMA) has enhanced the seismic network with permanent stations and ocean bottom seismometers. Seismic data are plentiful, and their quality is constantly enhanced. Research on earthquake relocation (Lavay-

ssière *et al.* 2022) has revealed the spatiotemporal distribution of seismic foci, identifying two seismic swarms: 1) a distal swarm that commenced as early as May 2018, characterised by earthquakes migrating upwards (from 40 to 20 km depth) and subsequently southwards (Cesca *et al.* 2020), and 2) a proximal swarm that began after June 2018. The former has a conical morphology (Lavayssière *et al.* 2022) and is situated under a caldera-like seabed configuration (Feuillet *et al.* 2021; REVOSIMA 2019), (Bhattacharya 2020).

Even though RGP noticed the strange movements of its four GNSS permanent stations as early as July 2018, it quickly became clear that keeping track of these changes required adding more GNSS stations and coordinating all related activities. In addition to the four previously used stations (MAYG, BDRL, GAMO, KAWÉ), two existing GNSS stations on the island from 2018 (MTSA and PORO) were employed for monitoring, along with three more stations particularly established in Mayotte in 2019 (KNKL, PMZI, and MTSB; Fig. 1a). A GNSS station (GLOR) was erected on Grande Glorieuse Island, about 250 km east-northeast of Mayotte. REVOSIMA used two supplementary stations, DSUA and NOSY, located north of Madagascar (about 400 km east of Mayotte), for the analysis of Mayotte data (Bousquet *et al.* 2020). However, these stations rapidly malfunctioned and have remained unrepaired due to the COVID-19 pandemic. Furthermore, no GNSS data exists for the other Comoros islands (Saurel *et al.* 2022; Peltier *et al.* 2022; REVOSIMA 2019).

The exhaustive inventory of GNSS stations used for monitoring the offshore eruption at Mayotte. All GNSS stations are linked to the internet via 4G networks or terrestrial links, enabling real-time querying. The four indigenous RGP stations (MAYG, BDRL, GAMO, KAWÉ) provide multi-GNSS observation hourly files with a 1-second sampling rate, while the remaining stations offer hourly or daily files at a 30-second sample rate. All observation data are converted into daily 30-second files for uniform processing. All groups involved in the network came together as a dedicated team starting in July 2018, led by IGN, to create a standard way of operating the stations and agree on how to centralise and share GNSS data and products, using the RGP infrastructure provided by IGN (Saurel *et al.* 2022; Peltier *et al.* 2022; REVOSIMA 2019).

The IGS station MAYG in East Africa is selected as the primary monitoring point for this study. This selection was strategic due to the proximity of MAYG to the equator, placing it within a more ionospherically active region. This location provides an opportunity to examine the latitude dependency of ionospheric delay differences, which can significantly im-

pact GNSS measurements. GNSS data from MAYG is obtained between 1 January 2014 and 1 January 2023 with observations recorded at a 30-second resolution. All RINEX (Receiver Independent Exchange Format) observations from MAYG are processed using CSRS-PPP AR Software, which is explained in detail below.

Data Processing Methods

Static processing method

Static GNSS surveying is widely implemented for calculating high-precision three-dimensional coordinates at fixed stations. This method delivers coordinate accuracy at the millimetre level in both horizontal and vertical components. Static positioning also enables precise azimuth determination, establishing network orientation relative to the reference system. A major advantage of GNSS-based surveying networks over traditional electromagnetic distance measuring devices is that they do not require inter-visibility between stations (Jackson, Kagan 2014). This characteristic makes GNSS particularly valuable for monitoring gravity field and geodynamic phenomena of the Earth such as polar motion, Earth tides, and crustal movements.

Kinematic processing method

In many surveying applications, speed and productivity are essential factors for success. Kinematic surveying represents the most productive form of satellite surveying, providing immediate coordinate values while the receiver is either stationary or in motion. Although kinematic surveys typically achieve less accuracy than static surveys, they remain adequate for most surveying applications, offering a practical balance between precision and efficiency.

Precise Point Positioning with Ambiguity Resolution (PPP-AR)

Precise Point Positioning with Integer Ambiguity Resolution (PPP-AR) has numerous applications, including deformation monitoring, co-seismic motion analysis, and precise tracking of movement on land, in air, at sea and in ionosphere (Ocalan *et al.* 2022; Ogutcu *et al.* 2023; Chen *et al.* 2024, 2025). The technique addresses a fundamental challenge in GNSS processing: the integer nature of initial carrier-phase ambiguity is compromised as it absorbs additional phase biases from receiver and transmitter hardware. These biases cannot be estimated simultaneously with ambiguities due to their one-to-one correlation. To overcome this limitation, a specific re-parameter-

ization approach enables phase bias estimation based on processing observations from global or regional continuously operating reference stations. When initial ambiguities are resolved as integer values, the solution quality improves in three key aspects such as enhanced accuracy, improved stability and reduced convergence period. The PPP-AR technique provides satellite clock and orbit corrections, components of Satellite-Specific Signals (SSRs) to user receivers (Naciri *et al.* 2024). This correction information is particularly relevant to algorithmic processing in our study.

The Canadian Geodetic Survey (CGS) of Natural Resources Canada (NRCan) (CanadianGeodeticSurvey 1909) updated the Canadian Spatial Reference System Precise Point Positioning (CSRS-PPP) service in October 2020 (CSRS-PPP 1983). This modernization includes PPP-AR capabilities for data collected from 1 January 2018 onward. Ambiguity resolution offers significant benefits by transforming ambiguous carrier-phase observations into precise ranges, enabling centimetre-level accuracies with faster acquisition times. Additionally, due to satellite geometry considerations, resolving carrier-phase ambiguities particularly enhances the longitude (east) component estimates (Atiz, Kalayci 2021; Bilgen *et al.* 2022; Mou *et al.* 2023; Konakoglu, Yilmaz 2024). It's important to note that prior to January 2018, there were insufficient analysis centres providing satellite phase biases consistent with satellites' orbits and clocks – data required for effective ambiguity resolution. This technical limitation informed our processing approach for pre-2018 data in this study.

RESULTS AND DISCUSSION

In this study, the differences of the horizontal and vertical components between kinematic and static processing are computed by years. To investigate the crustal deformation associated with the Mayotte volcanic and seismic crisis, the daily GNSS solutions are analyzed for the MAYG station, which provided continuous, high-quality measurements throughout the study period (2018–2021). Displacement time series in the east, north, and vertical components are computed relative to a stable CSRS-PPP reference frame. The resulting data are processed to extract both linear and non-linear trends in ground movement. The GNSS displacement vectors into seasonal segments are then decomposed to capture temporal shifts in direction and magnitude, focusing particularly on transitions that may reflect changes in magmatic or tectonic processes. By evaluating the evolution of these displacement vectors and correlating them with known geophysical events, such as variations in seismicity and eruptive activity, the underlying dynamics

driving the Mayotte crisis are better understood. The following section presents the observed deformation trends, vector orientation shifts, and their geophysical interpretations with emphasis on the turning point identified in mid-2019.

Figure 2 illustrates the comprehensive nine-year record (January 2014 to January 2023) of ground displacement at the MAYG station, providing crucial insights into the evolution of the Mayotte seismic-volcanic crisis. Panel (a) displays the horizontal displacement vectors, while panel (b) shows the vertical displacement time series, both referenced to the ITRF2014 frame. The horizontal displacement pattern reveals three distinct phases of movement. Prior to May 2018, the station exhibited a consistent north-eastward migration at a relatively modest rate, aligning with the regional tectonic setting. Following the onset of magmatic activity on 10 May 2018, a dramatic shift occurred in both direction and magnitude, with the station abruptly changing the course toward the east. This eastward movement persisted until June 2019, accumulating a substantial total displacement during this 13-month period – representing the most rapid horizontal deformation rate observed throughout the entire monitoring period. After June 2019, the horizontal displacement vector rotated again, returning to a north-easterly direction but maintaining an elevated displacement rate compared to the pre-crisis period. This sustained movement suggests ongoing magmatic processes beneath the seafloor, even as seismic activity diminished from its peak levels.

The vertical displacement record (Fig. 2b) reveals an equally striking pattern. From 2014 until May

2018, the station maintained a relatively stable vertical position with minor seasonal fluctuations. Following the onset of magmatic activity, however, a pronounced subsidence began, with the station sinking approximately 20 cm between May 2018 and June 2019. This rapid subsidence phase correlates precisely with the period of eastward horizontal movement, strongly suggesting a causal relationship between these displacement components. After June 2019, the rate of subsidence decreased significantly but did not entirely cease, with continuing but diminished vertical deformation through January 2023. This pattern mirrors the trend observed in the horizontal displacement components, reinforcing the interpretation of ongoing but reduced magmatic activity.

Figure 3 provides a focused examination of horizontal and vertical displacements at the MAYG station during the period from January 2014 through September 2018. This timeframe is particularly valuable as it captures both the pre-crisis baseline period and the initial response to the magmatic activity that began on 10 May 2018. Figure 4 zooms in on providing high-temporal resolution data during the critical five-day period immediately following the onset of magmatic activity (10–15 May 2018). This detailed view reveals the immediate response of the ground surface to the initiation of the seismic-volcanic crisis. Figure 5 extends the analysis into the prolonged phase of the crisis, covering September 2018 through January 2023. This longer-term view allows an assessment of how the deformation patterns evolved after the initial crisis phase and provides insight into the longer-term dynamics of the magmatic system.

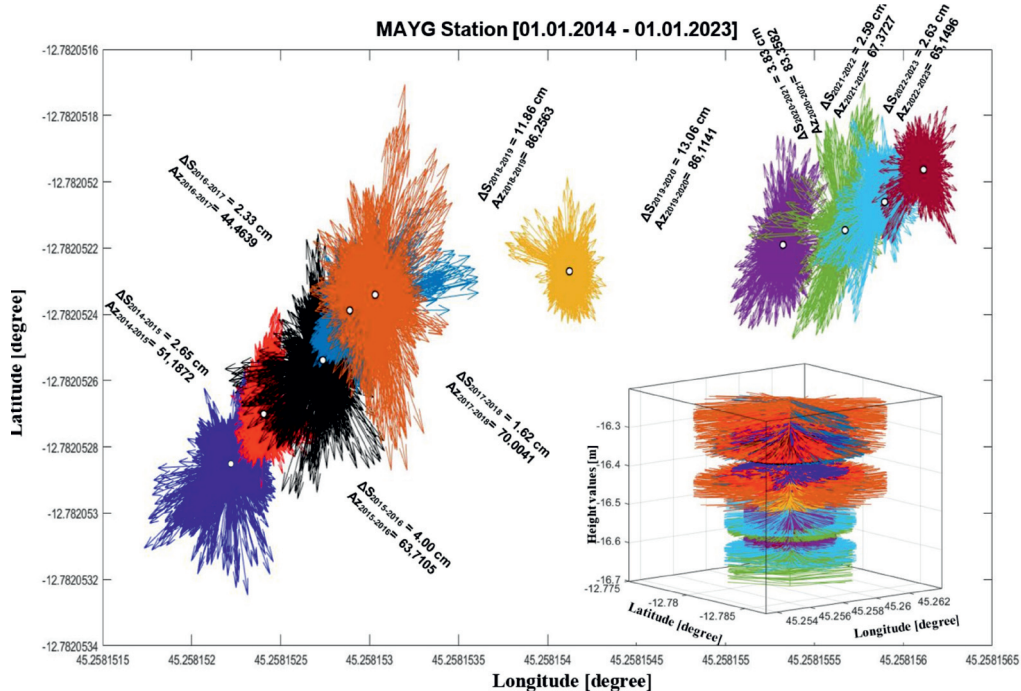


Fig. 2 Horizontal (a) and vertical (b) displacements of MAYG station between 1 January 2014 and 1 January 2023 (ITRF 2014)

In Fig. 3, the horizontal displacement pattern reveals a clear bifurcation point coinciding with the onset of magmatic activity. Prior to May 2018, the displacement vectors show a consistent north-eastward trend with relatively uniform magnitude and direction, indicating a stable regional tectonic influence. This steady-state motion establishes an important baseline against which the subsequent crisis-related deformation can be evaluated. Following the 10 May 2018 event, the horizontal displacement vectors show an abrupt change in direction, swinging from north-east to east, accompanied by a marked increase in the magnitude of displacement in Fig. 3. This directional shift represents the first geodetic evidence of the developing magmatic crisis and suggests an immediate response of the crustal material to subsurface pressure changes. The vertical component data in Fig. 3 similarly demonstrates a pronounced inflection point in May 2018. After maintaining relatively stable elevation with only minor fluctuations throughout the pre-crisis period, the MAYG station began experiencing significant subsidence following the onset of magmatic activity. This downward displacement accelerated through September 2018, indicating a rapid crustal response to the developing volcanic processes offshore.

In Fig. 4, the horizontal displacement vectors during this brief period show remarkable day-to-day variations in both direction and magnitude. This pattern

of rapidly changing displacement vectors suggests highly dynamic subsurface processes, likely reflecting the initial propagation of magma through new pathways in the crust. The inconsistent direction of these vectors may indicate complex stress redistributions as the magmatic system established its initial configuration. The vertical displacement data for this five-day period reveals an immediate subsidence response beginning from the very first day of the crisis. The accelerating downward trend during these five days provides crucial insight into the rapid mobilization of magmatic material. The correlation between the timing of these vertical displacements and the concurrent seismic swarm activity supports interpretations of a causal relationship between these phenomena. This high-resolution temporal view of the crisis initiation phase represents a unique dataset in volcano logical studies, capturing the immediate geodetic signature of a major submarine magmatic event during its earliest development stages. The height changes are approximately 20 cm (swell and collapse). The differences in height components on 10, 11, 12 May 2018 seem to be the precursor of the 13 May 2018 earthquake.

In Fig. 5, the horizontal displacement data reveals a gradual reorientation of movement vectors beginning around June 2019, when the predominantly eastward motion began shifting back toward a north-easterly direction. This directional change coincides with documented reductions in seismic activity and erup-

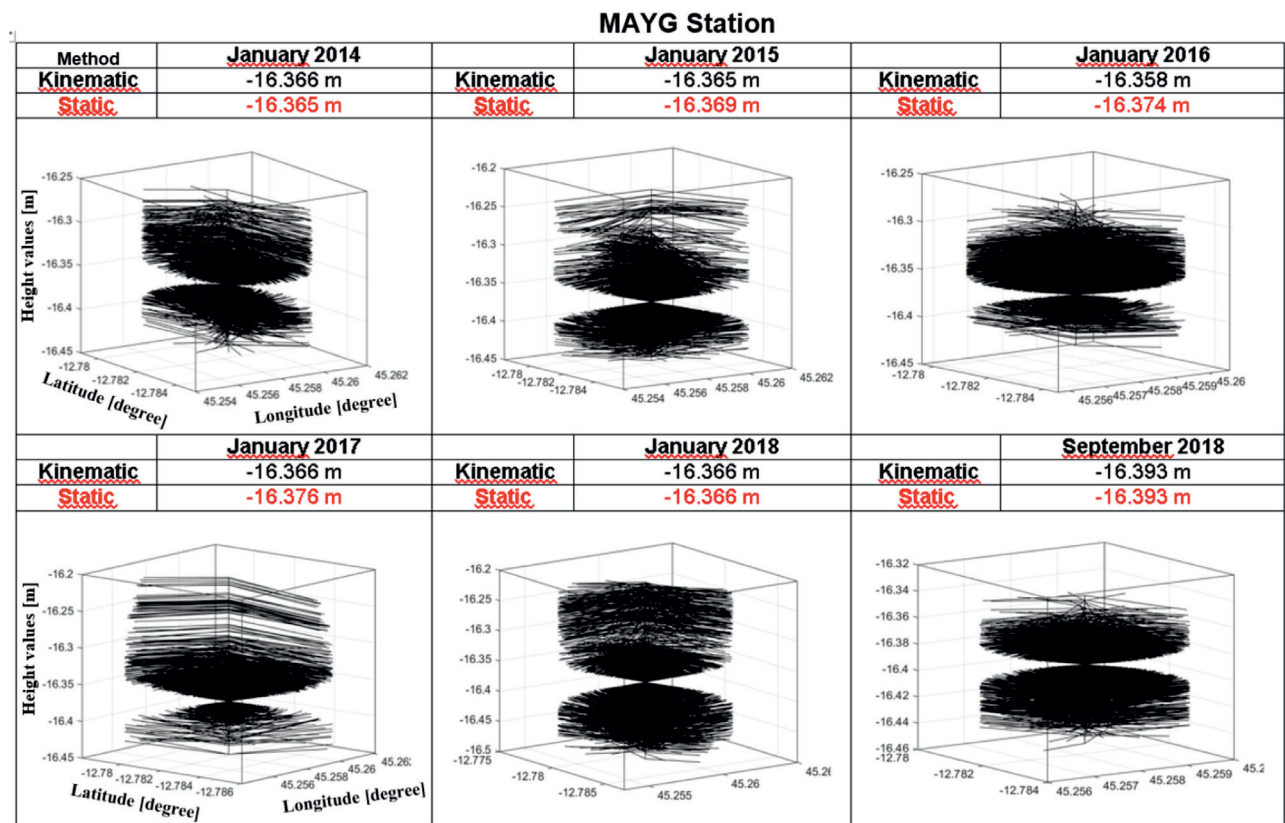


Fig. 3 The horizontal and vertical displacements of MAYG station between January 2014 and September 2018

MAYG Station

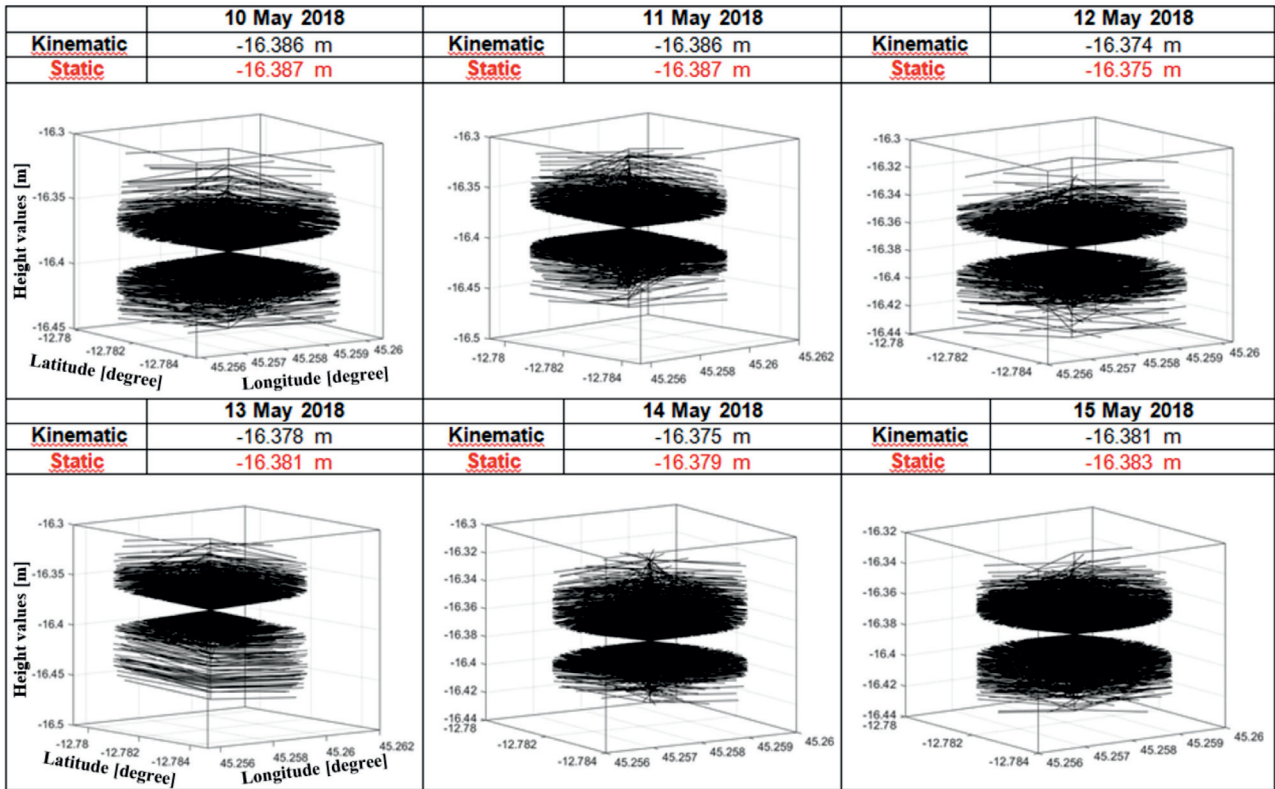


Fig. 4 The horizontal and vertical displacements of MAYG station between 10 May and 15 May 2018

MAYG Station

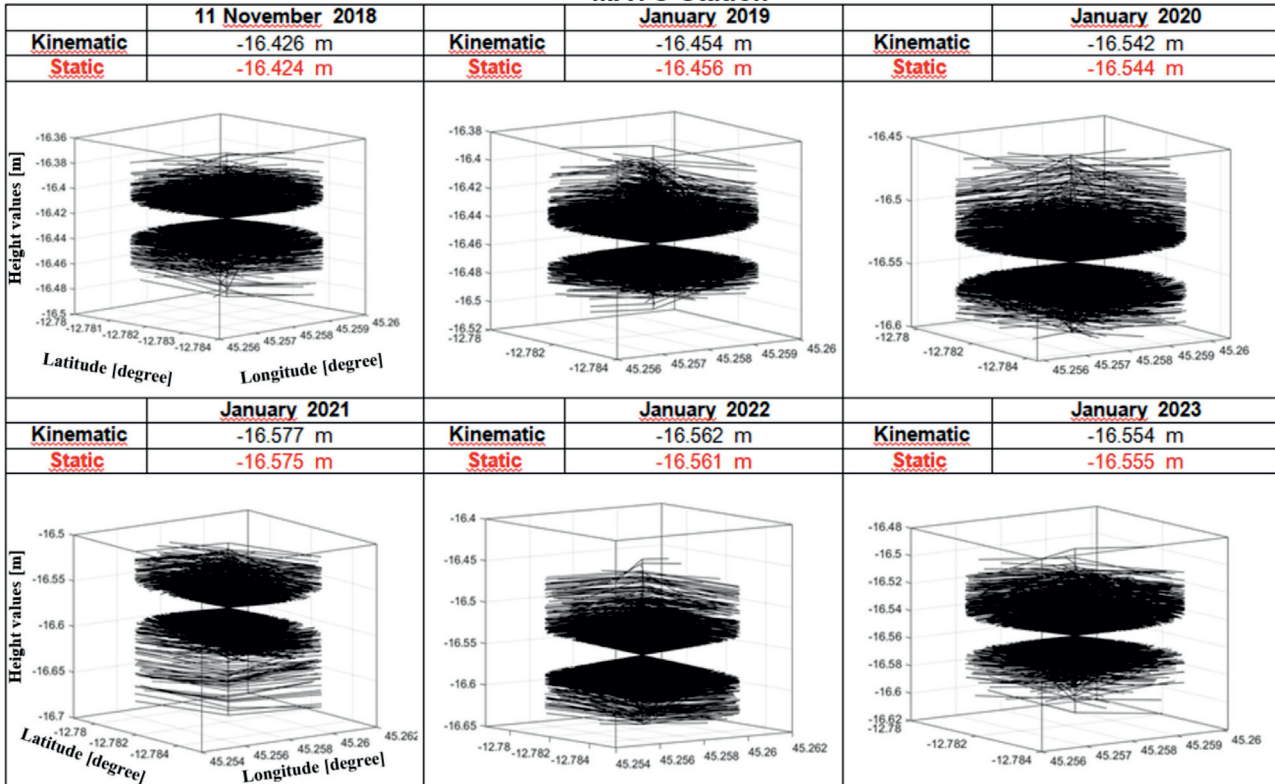


Fig. 5 The horizontal and vertical displacements of MAYG station between September 2018 and January 2023

tive flux at the submarine volcanic edifice. Despite this directional shift, the magnitude of horizontal displacement remained elevated compared to pre-crisis levels, indicating continued magmatic influence even as the system entered a less active phase. The vertical displacement component shows a similar transition, with the rapid subsidence that characterized the peak crisis period (May 2018 – June 2019) giving way to a slower but persistent downward trend. This continuing subsidence, albeit at reduced rates, suggests the ongoing mass transfer within the magmatic system even as surface expressions of activity diminished. The extended temporal coverage in Fig. 5 reveals that while the most dramatic deformation occurred during the first year of the crisis, the MAYG station continued to record a significant displacement through January 2023, indicating that the magmatic system remained active long after the peak crisis phase. As of 11 November 2018, the differences in the vertical direction have returned to their previous level (mm level). The horizontal displacement of the MAYG station is approximately 10.60 cm in the north-east direction from 2014 to 2018. Starting from 2018, this north-east movement has turned to the east direction because the earthquake swarm effect is 11.86 cm.

Figure 6 provides a detailed visualization of the coordinate variations at the MAYG station during the critical five-day period immediately following the onset of the magmatic activity on 10 May 2018. Panel (a) illustrates the two-dimensional coordinate variations, while panel (b) presents the three-dimensional coordinate variations resulting from the earthquake swarm. The two-dimensional representation in panel (a) reveals the complex, non-linear trajectory of horizontal displacement during this intense period of activity. Unlike the relatively uniform directional trends observed over longer time scales, this high-resolution view exposes rapid fluctuations in displacement direction and magnitude over extremely short time intervals. These abrupt changes in position likely reflect the station's response to individual significant seismic events within the swarm, each potentially representing discrete magma movement episodes or fault adjustments. The three-dimensional visualization in panel (b) adds crucial insight by incorporating the vertical component, demonstrating how the horizontal displacements correlate with simultaneous vertical position changes. This integrated view reveals that the periods of accelerated horizontal movement frequently coincided with more pronounced vertical displacement, suggesting a mechanically coupled response to the underlying processes. The three-dimensional trajectory appears to follow a complex path that cannot be explained by simple elastic deformation models, indicating a combination of multiple forcing mechanisms acting simultaneously on the crustal

material. The coordinate variations shown in Fig. 6 capture the chaotic nature of ground response during the initial crisis phase, revealing how the surface deformation during this period resulted from a complex interplay of seismic energy release and magmatic pressure changes. The irregular pattern suggests that during these first five days, the magmatic system was establishing pathways through the crust, resulting in distributed stress release rather than organized directional flow. Figure 7 provides an alternative three-dimensional representation of the coordinate variations at the MAYG station during the same five-day period following the onset of magmatic activity. This visualization technique offers an additional perspective on the spatial relationship between horizontal and vertical displacements during this critical phase. The three-dimensional trajectory depicted in Fig. 7 clearly demonstrates that the displacement was not confined to a single plane but rather explored a complex volume of space during the earthquake swarm. This volumetric pattern indicates that the station was responding to forces with varying directional components throughout the initial crisis period. Particularly notable is how the trajectory appears to form clusters or nodes at certain positions, suggesting periods of relative stability interrupted by sudden movements – a pattern consistent with stick-slip behaviour often associated with incremental fault adjustments or discrete magma intrusion events. The spatial distribution of the coordinate positions reveals an overall trend of movement away from the starting position, but with significant excursions from any simple direct path. This complex path geometry provides evidence that the initial response to the magmatic activity involved multiple mechanisms rather than a simple deflation or lateral translation process. The station appears to have experienced a combination of subsidence, lateral shift, and rotational components, indicating a complex stress field evolution during this period. The relationship between the horizontal and vertical components visualized in this three-dimensional space suggests that the initial phase of the crisis involved a sequence of distinct deformation events rather than a continuous process. This discretization provides valuable constraints for modelling the mechanics of the underlying magmatic system and suggests that the initial magma mobilization likely progressed through a series of distinct pulses or adjustments rather than as a continuous flow.

Figure 8 presents a comprehensive view of the MAYG station displacements spanning the entire study period from 2014 to 2023, with separate panels illustrating (a) three-dimensional displacement, (b) vertical displacement, and (c) horizontal displacement. This integrated visualization serves as a capstone representation of the complete temporal evolu-

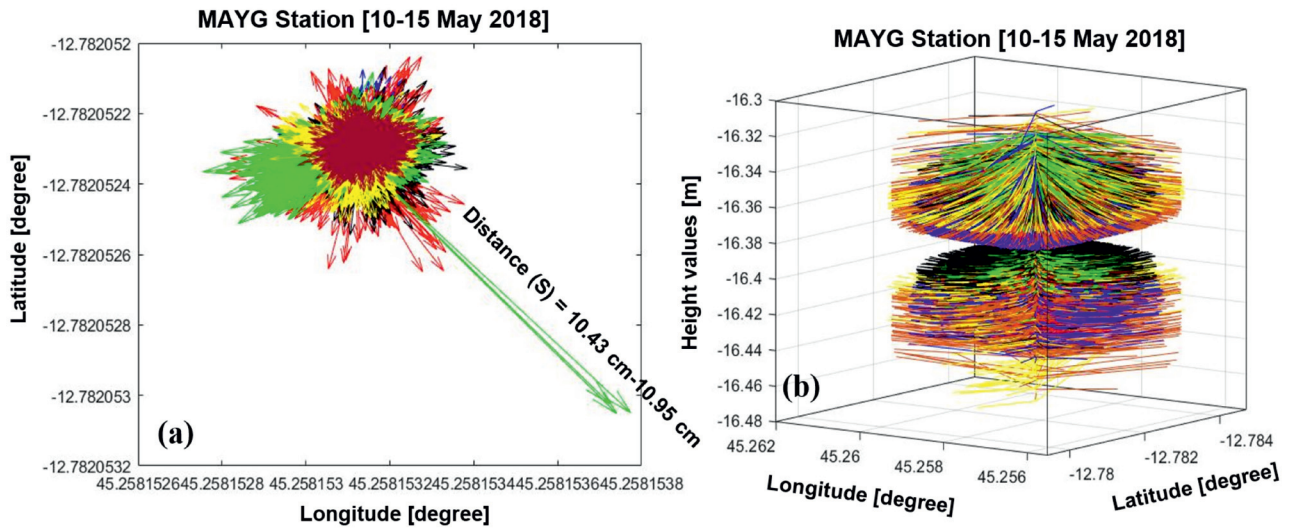


Fig. 6 Coordinate variations for MAYG station between 10 and 15 May 2018: two-dimensional coordinate variations (a) and three-dimensional coordinate variations due to the earthquake swarm (b)

tion of ground deformation throughout the pre-crisis, crisis, and post-crisis phases. The three-dimensional displacement trajectory in panel (a) provides a holistic spatial perspective on how the MAYG station position evolved over the nine-year monitoring period. This visualization effectively demonstrates that while the horizontal and vertical components are often analysed separately, they represent parts of a unified response to the underlying geophysical processes. The trajectory reveals three distinct phases: a period of relatively minor displacement during the pre-crisis years (2014 – early 2018), followed by a dramatic acceleration and directional change coinciding with the May 2018 magmatic event, and finally a prolonged but gradually moderating displacement phase extending through 2023. Panel (b), focusing on the vertical displacement component, illustrates with striking clarity the dramatic subsidence that began with the onset of magmatic activity. The vertical displacement time series shows minimal variation before May 2018, followed by a sharp downward trend that appears to occur in two phases—an initial rapid subsidence from May 2018 to approximately June 2019, followed by a more moderate but continuing downward trend through 2023. The total subsidence of approximately 20 cm represents a significant crustal response and provides strong constraints on the volume of magma withdrawal from beneath the island. The horizontal displacement represented in panel (c) mirrors this temporal pattern while revealing important directional characteristics. The pre-crisis period shows a modest north-eastward movement consistent with regional tectonic influences. Following the May 2018 magmatic onset, the horizontal displacement vectors show both increased magnitude and an eastward rotational component, pointing toward the

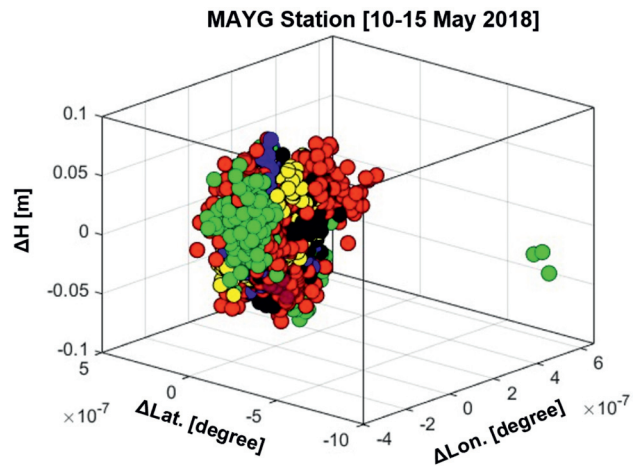


Fig. 7 Three-dimensional coordinate variations at the MAYG point due to the earthquake swarm in Mayotte Island between 10 and 15 May 2018

location of the offshore volcanic edifice. After June 2019, the vectors gradually rotate back toward a more north-easterly direction while maintaining elevated displacement rates compared to the pre-crisis period.

What is particularly valuable about Fig. 8 is how it integrates these displacement components to reveal their temporal correlation. The periods of most rapid horizontal displacement precisely coincide with the intervals of accelerated subsidence, strongly supporting the interpretation that both components are responding to the same underlying magmatic processes. The figure also demonstrates that while the crisis-related deformation has moderated since 2019, the MAYG station has not returned to its pre-crisis deformation pattern, suggesting a permanent alteration in the regional stress regime following this significant magmatic event. The nine-year record presented in Fig. 8 constitutes one of the most complete geodetic time

series ever obtained for a major submarine volcanic event. The continuous nature of the dataset, spanning pre-crisis, crisis, and extended post-crisis periods, provides unprecedented insight into the complete lifecycle of such an event. The ability to observe the transition from background deformation through crisis response and into a new post-event equilibrium state represents a significant contribution to our understanding of how island landmasses respond to off-shore magmatic processes.

The patterns revealed in Fig. 8 support the hypothesis that the directional changes in horizontal displacement, coupled with the significant vertical subsidence, reflect a complex magma extraction process beneath Mayotte, feeding the submarine eruption 50 km offshore. The persistent nature of the deformation through 2023, albeit at reduced rates, suggests that while the most dramatic phase of the event has passed, the magmatic system remains active and continues to influence crustal deformation

around Mayotte. This comprehensive view provides essential context for interpreting the more detailed temporal analyses presented in previous figures and establishes the Mayotte seismic-volcanic crisis as an event of exceptional duration and magnitude within the global record of monitored volcanic activity.

The observed transition in June 2019, marked by a shift in horizontal displacement back toward the northeast and a sharp decline in the rate of subsidence, likely reflects a major evolution in the magmatic system. This turning point coincides with a substantial reduction in seismicity and eruptive flux, suggesting that the primary phase of magma withdrawal had concluded. Geologically, this behaviour is consistent with the exhaustion or significant depletion of a deep magma reservoir beneath Mayotte, which had been feeding the offshore eruption since mid-2018. As the pressure within this reservoir decreased, the driving force behind rapid lateral and vertical crustal movements diminished. The subsequent deformation pat-

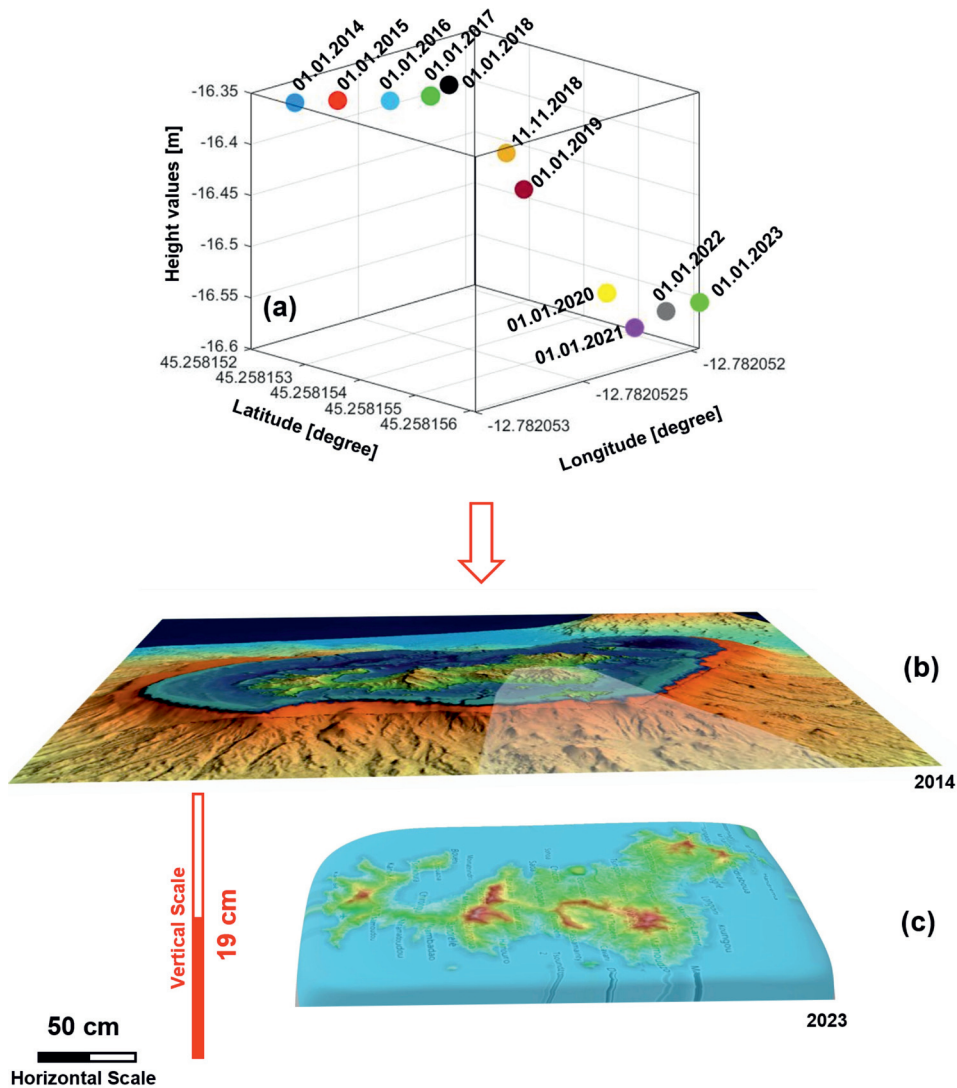


Fig. 8 The horizontal and vertical displacements of MAYG station between 2014 and 2023: three-dimensional displacement (a), vertical displacement (b) and horizontal displacement (c)

tern likely reflects residual adjustments in the crust – possibly due to viscoelastic relaxation or continued slow magma migration at depth – rather than active pressurization or rapid magma transport. This transition marks the system’s entry into a post-crisis adjustment phase, in which the crust responds to the new stress regime established after the main eruptive and intrusive events.

The temporal correlation between the abrupt changes in displacement patterns and the documented onset of magmatic activity on 10 May 2018 provides compelling evidence that these ground deformations directly result from magma migration processes. The eastward direction of horizontal displacement during the crisis phase points toward the offshore volcanic edifice approximately 50 km east of Mayotte, consistent with models suggesting magma extraction from a deep reservoir beneath the island feeding the submarine eruption. This extended time series significantly expands upon previous studies that focused primarily on the initial crisis period, allowing us to characterize the complete lifecycle of this exceptional geological event, from precursory signals through peak activity to the current state of diminished but persistent deformation. The clear directional changes observed in the horizontal displacement vectors, combined with the corresponding phases of vertical subsidence, provide strong constraints for modelling the underlying magmatic processes and offer new insights into the mechanics of submarine volcanic systems.

Figures 3, 4, and 5 provide a multi-scale temporal analysis of the Mayotte seismic-volcanic crisis, from the immediate response (days), through the early development phase (months), to the long-term evolution (years). This nested approach to temporal analysis reveals how initial rapid responses transitioned into sustained patterns of deformation, offering unprecedented insight into the lifecycle of a major submarine volcanic event. The progression from pre-crisis stability, through crisis-induced directional change, to post-peak readjustment demonstrates the dynamic nature of crustal response to magmatic processes. The consistent correlation between horizontal directional changes and vertical subsidence rates across all three temporal scales strengthens the interpretation that these displacement patterns directly reflect the underlying magmatic activity.

Figures 6 and 7 offer complementary perspectives on the same critical five-day period with Fig. 6 emphasizing the temporal evolution of the coordinate changes, while Fig. 7 highlights their spatial distribution. The integration of these visualizations reveals several key insights. The initial response to the magmatic activity was highly dynamic, with rapid changes in both direction and magnitude of displacement over very short time intervals. The deformation

process was a three-dimensionally complex, involving coupled horizontal and vertical movements that cannot be explained by simple deformation models. The coordinate changes appear to occur in discrete episodes rather than as a continuous process, suggesting a series of distinct mechanical adjustments in the subsurface. The overall pattern indicates an initial period of system adjustment as the magmatic processes established their primary pathways through the crust. These high-resolution data from the earliest days of the crisis provide unprecedented insight into the initial mechanics of a major submarine magmatic event. The complex patterns observed suggest that the early phases of such events involve complicated interactions between magma movement, fault slip, and elastic crustal response – interactions that are often overlooked in longer-term analyses that smooth out these short-duration features. Finally, the patterns shown in Fig. 8 lend credence to the theory that the substantial vertical subsidence and the directional shifts in horizontal displacement underlie a complicated magma extraction mechanism beneath Mayotte, which fuels the submarine eruption 50 kilometres offshore.

CONCLUSION

This study presents a comprehensive geodetic investigation of the unprecedented Mayotte seismic-volcanic crisis through long-term GNSS observations and advanced processing techniques, including static and kinematic positioning as well as PPP-AR. By analysing a continuous nine-year time series (2014–2023) from the MAYG GNSS station, we successfully identified distinct phases of ground deformation that correspond closely with the timeline of magmatic activity initiated in May 2018. A key contribution of this work lies in revealing temporal shifts in displacement vector orientation, particularly the abrupt transition from a north-eastward trajectory to an eastward movement coinciding with the onset of the crisis. This directional change, followed by a return to the pre-crisis trend after June 2019, reflects evolving stress regimes and dynamic magma migration processes beneath the island. Furthermore, the vertical component analysis exposed approximately 20 cm of subsidence between May 2018 and June 2019, providing strong geophysical evidence for magma withdrawal from a deep reservoir, possibly feeding the newly discovered submarine volcano 50 km offshore.

The deformation patterns observed in the earliest days of the crisis – characterized by rapid and complex coordinate shifts – suggest a mechanically coupled crustal response to deep magmatic intrusion and fault readjustment. These findings are reinforced by the three-dimensional trajectory visualizations, which indicate that the crustal deformation cannot be

explained by simple elastic models, but instead likely involves a combination of fault slip, magma pressure variations, and viscoelastic relaxation. By leveraging both static and kinematic GNSS processing, along with recent advancements in ambiguity-resolved PPP solutions, our study achieved centimetre-level precision in quantifying displacement. This methodological rigor enabled the identification of subtle yet geophysical significant transitions in crustal behaviour over time.

Importantly, this research enhances our understanding of submarine volcanic systems – particularly those occurring at considerable depths – and their potential to induce long-term crustal adjustments on adjacent islands. The persistent deformation recorded through 2023 suggests that the magmatic system beneath Mayotte remains active, warranting continued geodetic and seismic monitoring to assess future risks. Overall, the study not only contributes valuable insights into the mechanics of the Mayotte event but also underscores the critical role of continuous, high-resolution geodetic surveillance in interpreting complex volcanic processes and improving early warning frameworks for tectonically active island regions.

ACKNOWLEDGEMENTS

The authors would like to sincerely thank the Reviewers for their helpful feedback and recommendations, which have greatly improved the quality of this work. For their careful direction and professional management of the review process, the authors also want to express their sincere gratitude to the Journal Editors.

REFERENCES

- Aiken, C., Saurel, J.-M., Foix, O. 2021. Earthquake location and detection modeling for a future seafloor observatory along Mayotte's volcanic ridge. *Journal of Volcanology and Geothermal Research* 418, 1–12. <https://doi.org/10.1016/j.jvolgeores.2021.107322>
- Atiz, O.F., Kalayci, I. 2021. Performance Assessment of PPP-AR Positioning and Zenith Total Delay Estimation with Modernized CSRS-PPP. *Artificial Satellites* 56, 18–34. <https://doi.org/10.2478/arsa-2021-0003>
- Bertil, D., Mercury, N., Doubre, C., Lemoine, A., Wöer, J.V. 2021. The unexpected Mayotte 2018–2020 seismic sequence: a reappraisal of the regional seismicity of the Comoros. *Comptes Rendus Géoscience* 353, 211–235. <https://doi.org/10.5802/crgeos.79>
- Bhattacharya, S. 2020. Source of unusual monochromatic wave packets recorded globally in the seismograms of 11 November 2018. *Current Science* 118(7), 1069–1076. [doi:10.18520/cs/v118/i7/1069-1076](https://doi.org/10.18520/cs/v118/i7/1069-1076)
- Bilgen, B., Bulbul, S., Inal, C. 2022. Statistical Comparison on Accuracies of Web-Based Online PPP Services. *Journal of Surveying Engineering* 148(4), 1–11. [https://doi.org/10.1061/\(ASCE\)SU.1943-5428.000040](https://doi.org/10.1061/(ASCE)SU.1943-5428.000040)
- Bousquet, O., Lees, E., Durand, J., Peltier, A., Duret, A., Mekies, D., Boissier, P., Donal, T., Fleischer-Dogley, F., Zakariasy, L. 2020. Densification of the Ground-Based GNSS Observation Network in the Southwest Indian Ocean: Current Status, Perspectives, and Examples of Applications in Meteorology and Geodesy. *Frontiers in Earth Science* 8, 1–9. <https://doi.org/10.3389/feart.2020.566105>
- Cesca, S., Letort, J., Razafindrakoto, H.N.T., Heimann, S., Rivalta, E., Isken, M.P., Dahm, T. 2020. Drainage of a deep magma reservoir near Mayotte inferred from seismicity and deformation. *Nature Geoscience* 13(1), 87–93. [doi:10.1038/s41561-019-0505-5](https://doi.org/10.1038/s41561-019-0505-5)
- Chen, Z., Luo, X., Li, Y. 2024. Performance of kinematic GPS PPP AR under different ionospheric scintillation conditions. *Advances in Space Research* 73(6), 3098–3115. <https://doi.org/10.1016/j.asr.2023.12.065>
- Chen, Z., Luo, X., Liang, X., Li, Y., Lin, Y., Bian, S. 2025. Comprehensive analysis of different GNSS receivers performance based on PPP-AR and positioning accuracy during 22 geomagnetic storms in 2023. *Advances in Space Research* 75(4), 3630–3650. <https://doi.org/10.1016/j.asr.2024.11.067>
- Devès, M.H., Moirand, S., Vagueresse, L.L., Robert, G. 2022. Mayotte's seismo-volcanic “crisis” in news accounts (2018–2021). *Comptes Rendus Géoscience* 354, 391–415. <https://doi.org/10.5802/crgeos.149>
- Dolchinkov, N. 2024. Natural Emergencies and Some Causes of Their Occurrence: a Review. *Trends in Ecological and Indoor Environmental Engineering* 2(1), 18–27. <https://doi.org/10.62622/TEIEE.024.2.1.18-27>
- Fabris, M., Floris, M. 2023. Editorial for Special Issue “Ground and Structural Deformations Monitoring Systems Integrating Remote Sensing and Ground-Based Data. *Remote Sensing* 15(12), 1–6. <https://doi.org/10.3390/rs15123013>
- Fan, T., Wang, Y., Sun, L., Wang, P., Hou, J. 2024. A Review of Historical Volcanic Tsunamis: A New Scheme for a Volcanic Tsunami Monitoring System. *Journal of Marine Science and Engineering* 12(2), 1–13. <https://doi.org/10.3390/jmse12020278>
- Feuillet, N., Jorry, S., Crawford, W.C., Deplus, C., Thinon, I., et al. 2021. Birth of a large volcanic edifice offshore Mayotte via lithosphere-scale dyke intrusion. *Nature Geoscience* 14, 787–795. <https://doi.org/10.1038/s41561-021-00809-x>
- Foix, O., Aiken, C., Saurel, J.-M., Feuillet, N., Jorry, S.J., Rinnert, E., Thinon, I. 2021. Offshore Mayotte volcanic plumbing revealed by local passive tomography. *Journal of Volcanology and Geothermal Research* 420, 1–14. <https://doi.org/10.1016/j.jvolgeores.2021.107395>
- Gagliardi, V., Tosti, F., Bianchini Ciampoli, L., Battagliere, M., D'Amato, L., Alani, A., Benedetto, A. 2023. Satellite Remote Sensing and Non-Destructive Testing Methods for Transport Infrastructure Monitoring: Advances, Challenges and Perspectives. *Remote Sensing*

- 15(2), 1–29. <https://doi.org/10.3390/rs15020418>
- Jackson, D.D., Kagan, Y.Y. 2014. Characteristic Earthquakes and Seismic Gaps. In: *Encyclopedia of Solid Earth Geophysics* 37–40. Dordrecht: Springer. https://doi.org/10.1007/978-90-481-8702-7_181
- Janson, M., Anthony, E.J., Charroux, S., Aubry, A., Dolique, F. 2021. Detecting the effects of rapid tectonically induced subsidence on Mayotte Island since 2018 on beach and reef morphology, and implications for coastal vulnerability to marine flooding. *Geo-Marine Letters* 41, 1–10. <https://doi.org/10.1007/s00367-021-00725-4>
- Konakoglu, B., Yilmaz, V. 2024. Evaluating the Performance of the Static PPP-AR in a Forest Environment. *Journal of Surveying Engineering* 150(2), 1–11. <https://doi.org/10.1061/JSUED2.SUENG-1403>
- Lacombe, T., Gurioli, L., Muro, A.D., Médard, E., Berthod, C., Bachèlery, P., Komorowski, J.-C. 2024. Late Quaternary explosive phonolitic volcanism of Petite-Terre (Mayotte, Western Indian Ocean). *Bulletin of Volcanology* 86, 1–36. <https://doi.org/10.1007/s00445-023-01697-2>
- Lavayssi'ere, A., Crawford, W.C., Saurel, J.M., Satriano, C., Feuillet, N., Jacques, E., Komorowski, J.C. 2022. A new 1D velocity model and absolute locations image the Mayotte seismo-volcanic region. *Journal of Volcanology and Geothermal Research* 421, 107440. <https://doi.org/10.1016/j.jvolgeores.2021.107440>
- Lemoine, A., Briole, P., Bertil, D., Roullé, A., Foumelis, M., Thinon, I., Raucoules, D., de Michele, M., Valt, P., Colomer, R.H. 2020. The 2018–2019 seismo-volcanic crisis east of Mayotte, Comoros islands: seismicity and ground deformation markers of an exceptional submarine eruption. *Geophysical Journal International* 223(1), 22–44. <https://doi.org/10.1093/gji/ggaa273>
- Liuzzo, M., Muro, A.D., Rizzo, A.L., Caracausi, A., Grassa, F., Fournier, N., Italiano, F. 2021. Gas Geochemistry at Grande Comore and Mayotte Volcanic Islands (Comoros Archipelago), Indian Ocean. *Geochemistry, Geophysics, Geosystems* 22(8), 1–43. <https://doi.org/10.1029/2021GC009870>
- Mercury, N., Lemoine, A., Doubre, C., Bertil, D. 2023. Onset of a submarine eruption east of Mayotte, Comoros archipelago: the first ten months seismicity of the seismo-volcanic sequence (2018–2019). *Comptes Rendus Géoscience* 354(2022), 105–136. <https://doi.org/10.5802/crgeos.191>
- Mittal, T., Jordan, J.S., Retailleau, L., Beauducel, F., Peltier, A. 2022. Mayotte 2018 eruption likely sourced from a magmatic mush. *Earth and Planetary Science Letters* 590, 1–13. <https://doi.org/10.1016/j.epsl.2022.117566>
- Mori, M. 2021. Crisis narratives and (dis)placement: Space, time and earthquakes in Mayotte. *Ampersand* 8, 1–9. <https://doi.org/10.1016/j.amper.2021.100078>
- Mou, Y., Luo, X., Xie, Z., Peng, X. 2023. Performance analysis of four PPP service software under different intensity geomagnetic storms. *Advances in Space Research* 72(5), 1593–1604. <https://doi.org/10.1016/j.asr.2023.04.026>
- Naciri, N., Bisnath, S., Wübbena, G., Wübbena, J., Schmitz, M., Vachlavovic, P., Capua, R. 2024. GNSS PPP-AR utilizing local SSR corrections. *GPS Solutions* 28 1–15. <https://doi.org/10.1007/s10291-024-01757-w>
- Nagashima, F., Kawase, H., Nakano, K., Ito, E. 2023. Estimation of weak and strong ground motions based on diffuse field concept for earthquake for steps 2 and 3 of blind prediction exercise. *Earth, Planets and Space* 75(104), 1–17. <https://doi.org/10.1186/s40623-023-01859-8>
- Necmioglu, O., Heidarzadeh, M., Vougioukalakis, G.E., Selva, J. 2023. Landslide Induced Tsunami Hazard at Volcanoes: the Case of Santorini. *Pure and Applied Geophysics* 180, 1811–1834. <https://doi.org/10.1007/s00024-023-03252-8>
- Neris, J., Robichaud, P., Wagenbrenner, J., Brown, R., Doerr, S. 2023. Soil erosion after fire in volcanic terrain: Assessment and implications for post-fire soil losses. *Journal of Hydrology*, 625(A), 1–14. <https://doi.org/10.1016/j.jhydrol.2023.129923>
- Noviyanto, A., Sartohadi, J., Purwanto, B.H. 2020. The distribution of soil morphological characteristics for landslide-impacted Sumbing Volcano, Central Java – Indonesia. *Geoenvironmental Disasters* 7, 1–19. <https://doi.org/10.1186/s40677-020-00158-8>
- Ocalan, T., Turk, T., Tunalioglu, N., Gurturk, M. 2022. Investigation of accuracy of PPP and PPP-AR methods for direct georeferencing in UAV photogrammetry. *Earth Science Informatics* 15, 2231–2238. <https://doi.org/10.1007/s12145-022-00868-7>
- Ogutcu, S., Alcaay, S., Duman, H., Ozdemir, B. N., Konukseven, C. 2023. Static and kinematic PPP-AR performance of low-cost GNSS receiver in monitoring displacements. *Advances in Space Research* 72(11), 4795–4808. <https://doi.org/10.1016/j.asr.2023.09.025>
- Omira, R., Baptista, M., Quartau, R., Ramalho, R., Kim, J., Ramalho, I., Rodrigues, A. 2022. How hazardous are tsunamis triggered by small-scale mass-wasting events on volcanic islands? New insights from Madeira – NE Atlantic. *Earth and Planetary Science Letters* 578, 1–12. <https://doi.org/10.1016/j.epsl.2021.117333>
- Peltier, A., Saur, S., Ballu, V., et al. 2022. Ground deformation monitoring of the eruption off-shore Mayotte. The Mayotte seismo-volcanic crisis of 2018–2021 in the Comoros archipelago. *Comptes Rendus Géoscience* 354(2022), 171–193. <https://doi.org/10.5802/crgeos.176>
- Retailleau, L., Saurel, J.-M., et al. 2022. Automatic detection for a comprehensive view of Mayotte seismicity. *Comptes Rendus Géoscience* 354(2022), 153–170. <https://doi.org/10.5802/crgeos.133>
- Roullé, A., Baillet, M., Bertil, D., Cornou, C. 2022. Site effects observations and mapping on the weathered volcanic formations of Mayotte Island. *Comptes Rendus. Géoscience* 354, 317–341. <https://doi.org/10.5802/crgeos.151>
- Saurel, J.-M., Jacques, E., et al. 2022. Mayotte seismic crisis: building knowledge in near real-time by combin-

- ing land and ocean-bottom seismometers, first results. *Geophysical Journal International* 228(2), 1281–1293. <https://doi.org/10.1093/gji/ggab392>
- Shults, R., Ormambekova, A., Medvedskij, Y., An-nenkov, A. 2023. GNSS-Assisted Low-Cost Vi-sion-Based Observation System for Deforma-tion Monitoring. *Applied Sciences* 13(5), 1–36. <https://doi.org/10.3390/app13052813>
- Tan, D., Li, A., Ji, B., Duan, J., Tao, Y., Luo, H. 2023. Ground Deformation Monitoring for Subway Struc-ture Safety Based on GNSS. *Buildings* 13(11), 1–21. <https://doi.org/10.3390/buildings13112682>
- Vij, R. 2022. Types of Disasters. In: *Management of Ani-mals in Disasters* 3–14. Singapore: Springer.
- Yao, S., Yang, H. 2023. Towards ground motion prediction for potential large earthquakes from interseismic lock-ing models. *Earth and Planetary Science Letters* 601, 117905. <https://doi.org/10.1016/j.epsl.2022.117905>
- Yunita, F.T., Soekarno, I., Nugroho, J., Santosa, U.B. 2024. Empirical model for predicting erosion on slope covered by unconsolidated tephra. *Sadhana Acad-emy Proceedings in Engineering Sciences* 49, 1–16. <https://doi.org/10.1007/s12046-024-02456-5>
- Zinke, J., Reijmer, J., Thomassin, B., Dullo, W.-C., Grootes, P., Erlenkeuser, H. 2003. Postglacial flooding history of Mayotte Lagoon (Comoro Archipelago, south-west Indian Ocean). *Marine Geology* 194(3–4), 181–196. [https://doi.org/10.1016/S0025-3227\(02\)00705-3](https://doi.org/10.1016/S0025-3227(02)00705-3)
- Internet sources**
- Canadian Geodetic Survey. 1909. *Canadian Spatial Refer-ence System*. Retrieved 04-07-2025, from [https://natu-ral-resources.canada.ca/science-data/science-research/geomatics/geodetic-reference-systems/canadian-spa-tial-reference-system-csrs](https://natural-resources.canada.ca/science-data/science-research/geomatics/geodetic-reference-systems/canadian-spa-tial-reference-system-csrs)
- CSRS-PPP. 1983. *Canadian Spatial Reference System Precise Point Positioning*. Retrieved 04-07-2025, from <https://natural-resources.canada.ca/maps-tools-publi-cations/data>
- IGS. 1994. *International GNSS Service*. Retrieved 04-05-2025, from <https://network.igs.org/>
- REVOSIMA. 2019. Bulletin de l’activité sismo-volcanique à Mayotte, Technical Report ISSN: 2680-1205, IPGP/ BRGM/IFREMER/CNRS. Available online at: www.ipgp.fr/revosima (<https://www.ipgp.fr/en/research/phds/modeling-local-stresses-and-deep-structures-associated-with-seismicity-and-volcanism-offshore-mayotte/>).
- USGS. 1879. *United States Geological Survey*. Retrieved 04 03, 2025, from <https://www.usgs.gov/>
- VolcanoDiscovery. 2004. *Volcano Discovery*. Retrieved 04-07-2025, from <https://www.volcanodiscovery.com/mayotte-island.html>